Environmental Science & Technology

pubs.acs.org/est

Article

Extraction and Quantification of Nanoparticulate Mercury in Natural Soils

Weiping Cai, Yujun Wang, Yu Feng, Peng Liu, Shuofei Dong, Bo Meng, Hua Gong, and Fei Dang*

Cite This: *Environ. Sci. Technol.* 2022, 56, 1763−1770

Read Online

ACCESS | Metrics & More | Article Recommendations | Supporting Information

ABSTRACT: Nanoparticulate mercury (Hg-NPs) are ubiquitous in nature. However, the lack of data on their concentration in soils impedes reliable risk assessments. This is due to the analytical difficulties resulting from low ambient Hg concentrations and background interferences of heterogeneous soil components. Here, coupled to single particle inductively coupled plasma-mass spectrometry (spICP-MS), a standardized protocol was developed for extraction and quantification of Hg-NPs in natural soils with a wide range of properties. High particle number-, particle mass-, and total mass-based recoveries were obtained for spiked HgS-NPs (74−120%). Indigenous Hg-NPs across soils were within 10^7−10^{11} NPs g^{-1}, corresponding to 3−40% of total Hg on a mass basis. Metacinnabar was the primary Hg species in extracted samples from the Wanshan mercury mining site, as characterized by X-ray absorption spectroscopy and transmission electron microscopy. In agreement with the spICP-MS analysis, electron microscopy revealed comparable size distribution for nanoparticles larger than 27 nm. These indigenous Hg-NPs contributed to 5−65% of the measured methylmercury in soils. This work paves the way for experimental determinations of indigenous Hg-NPs in natural soils, which is critical to understand the biogeochemical cycling of mercury and thereby the methylation processes governing the public exposure to methylmercury.

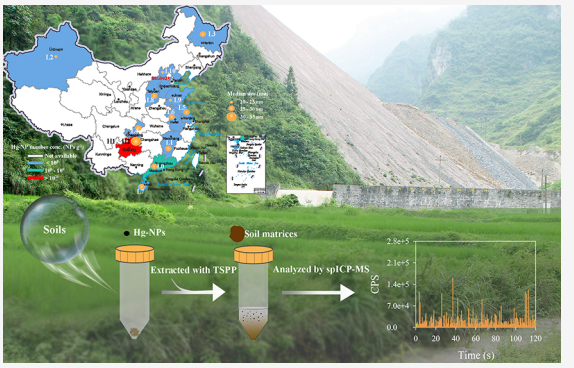

KEYWORDS: *mercury, nanoparticles, particle number, soils, extraction*

INTRODUCTION

Methylmercury (MeHg) is a potent neurotoxin that biomagnifies in the food chain and poses a global public health concern. Its production is largely determined by the bioavailability of inorganic mercury to microbial methylators. Particulate mercury, one of the most abundant inorganic mercury forms, is ubiquitous in various environmental matrices in oxic and anoxic settings.[1−6] Past efforts on particulate mercury have relied on methylation potentials using spiked particles.[7−10] These particles offer a wide range of reactivity and availability to methylators in pure cultures of bacteria, soils, and sediments,[7−10] due to their differences in particle size, crystal structure, dissolution, sorption, aggregation, and particle−cell interactions.[9−12] Especially, particulate mercury smaller than 100 nm, referred to as Hg-NPs, are of great concern due to their relatively high methylation potentials when compared to micro- and bulk Hg.[7,8] However, evidence for the exposure concentrations of indigenous Hg-NPs in complex soil matrices is limited. Very recently, Xu et al.[1] have shown that half of the Hg in the <0.5 μm size fraction of a contaminated marine sediment presents as individual mercury sulfide nanoparticles; yet, the number concentrations of indigenous Hg-NPs in natural soils remain largely unknown. The absence of these data hampers reliable risk assessments of Hg-NPs in environmentally relevant scenarios, including their actual role in MeHg production. This is primarily because of the lack of appropriate analytical methods.

Chemical identification of target Hg-NPs in complex soil matrices is not straightforward due to low concentrations of mercury (microgram per kilogram) and background interferences of heterogeneous soil components. Quantifying their number concentrations is even more challenging. Methods such as scanning and transmission electron microscopy could deliver qualitative or semiquantitative information on nanoparticles but require high mercury concentration (milligram per kilogram) to produce statistically reliable results.[13,14] Field-flow fractionation or liquid chromatography is adopted for particle size determination but is challenged by particle number concentration.[15,16] Single particle inductively coupled plasma-mass spectrometry (spICP-MS) is a promising technique to identify and quantify nanoparticles (e.g., Ag,

Received: October 15, 2021
Revised: December 24, 2021
Accepted: December 29, 2021
Published: January 10, 2022

https://doi.org/10.1021/acs.est.1c07039
Environ. Sci. Technol. 2022, 56, 1763−1770

Au, Fe, Zn, Ce, Ti, and Hg-containing NPs) in soils and sediments.[1,17−21] In addition to discrimination of particulate and dissolved forms in environmental samples, it offers simultaneous information on particle number/mass concentrations and size distribution.[22−24] An important issue of spICP-MS analysis is the extraction of NPs from soil solid matrices. Indeed, recent studies have employed various extraction methods (e.g., ultrapure water, sodium nitrate, and tetrasodium pyrophosphate)[1,17,19]; yet, the lack of data validation across different soil types or the lack of comparability for data among different analytical techniques (e.g., transmission electron microscopy or X-ray absorption spectroscopy) makes the measured values challenge for the risk assessment.[18] Therefore, it is beneficial to develop a standardized method for Hg-NP extraction that is suitable for subsequent spICP-MS analysis across soils with a wide range of properties.

To tackle these challenges in quantifying indigenous Hg-NPs in natural soils, a systematic and generic method including the extraction and quantification of Hg-NPs is developed. This is accompanied by comparing the soil extraction efficiency of different reagents and validating the applicability of the proposed method across soils with a wide range of properties (i.e., pH, soil organic matter content, and ambient total mercury levels). Characterization of Hg-NPs in soils from the mercury mining site by transmission electron microscopy coupled with energy-dispersive X-ray spectroscopy (TEM-EDS) and X-ray absorption spectroscopy allows for the validation of spICP-MS results. The determination of Hg-NP number/mass concentrations and size distribution is critical to understand the geochemical fate of mercury and their ecotoxicological consequences in real environment.

MATERIALS AND METHODS

Nanoparticles and Characterization. Mercury sulfide nanoparticles used for spike recovery experiments were synthesized as described previously.[25] Briefly, 0.016 g of elemental sulfur (Jiancheng Biotechnology Co. Ltd., Nanjing, China) and 0.17 g of $Hg(NO_3)_2$ (Sigma-Aldrich) were added into 550 mL of ethylene glycol (Jiancheng Biotechnology Co. Ltd., Nanjing, China) containing 0.15 g of poly-(vinylpyrrolidone) (as the capping agent; Aladdin, China). The mixture was stirred for 2 h (10 rpm) in the dark at 125 °C. After cooling at room temperature (RT), the mixture was centrifuged at 11 000*g* for 15 min. The pellets were washed with ultrapure water (18.2 MΩ cm^{-1}, Millipore) and ethanol thoroughly to remove the adsorbed ethylene glycol. These nanoparticles (hereinafter referred to as HgS-NPs) were dispersed in ultrapure water and stored at 4 °C in dark for further analysis.

The crystalline structure of synthesized HgS-NPs was evaluated by X-ray diffraction (XRD, Rigaku Ultima IV diffractometer with a Cu Kα source). The morphology, size, and elemental composition of HgS-NPs were determined by transmission electron microscopy (TEM; JEOL JEM-2100, Japan) coupled with an energy-dispersive X-ray detector (EDS; X-max 65T, Oxford) at an accelerating voltage of 200 kV. Particle size distribution was assessed by randomly sampling 350 particles from TEM images using the Nano Measure software.

Soils. Thirteen soil samples were collected at 0−15 cm at the surface. They were selected based on their distinct soil properties and ambient total Hg levels, including (i) soils at low ambient Hg levels less than 136.7 $\mu g\ kg^{-1}$ (dw) (L0−L10) and (ii) soils at 45.7 and 357.1 mg kg^{-1} from the Wanshan mining site, the world's third largest Hg mine (H1 and H2).[26] All soils were air-dried, ground, sieved through a <0.15 mm mesh, and stored at RT until further use.[17,19] Total mercury, methylmercury (MeHg), and soil properties including pH, cation exchange capacity, soil organic matter content, and total sulfur are listed in Table S1.

Spike Recovery Experiments. Particle extraction without changing particle properties is a critical consideration for nanoparticle determination in soils. As no reference material, i.e., soil with known particle number and size distribution of Hg-NPs, is available, spike recovery experiments were performed. Synthesized HgS-NPs (100 μL) were added to different soils to achieve final Hg concentrations of 0.4 (soils L0−L10), 6.5 (H1), and 10.0 (H2) mg kg^{-1} (dw). After thoroughly mixing, soils were aged at RT for 24 h or up to 30 days (i.e., soil L0 at 0.4 mg kg^{-1}) to reach steady-state conditions.[27]

A schematic diagram of soil extraction experiments is provided in Figure S1. The extraction method was initially developed using 0.5 mM tetrasodium pyrophosphate (TSPP), 0.5 mM sodium thiosulfate ($Na_2S_2O_3$), 0.5 mM 2,3-dimercaptopropanesulfonate sodium salt (DMPS), and 0.01 mM sodium nitrate ($NaNO_3$) in soil L0. TSPP could disperse/dissolve soil organic matter adsorbed onto particle surfaces and disperse soil particles.[17,19] DMPS and $Na_2S_2O_3$ are strong chelators for Hg,[28] and $NaNO_3$ is used as a proxy for mimicking *in situ* soil pore water.[17] Afterward, the effect of TSPP concentrations (0.05−25 mM) was examined. Briefly, all extractions were performed in a reciprocal shaker at 200 rpm for 70 min (RT). After extraction, samples were water bath sonicated for 15 min (40 kHz), agitated vigorously, and allowed for a 2 h sedimentation at RT. To investigate the robustness and effectiveness of the extraction method, indigenous Hg-NPs in soil H1 were extracted in a first step (single extraction), followed by a second step of extraction using the same protocols (repeated extraction). Subsamples of the supernatant were collected and diluted for subsequent spICP-MS and total mercury analysis.

To validate the applicability of the extraction method established in soil L0, spike recovery experiments were conducted in soils L1−L10 and H1−H2. Nonspiked samples were studied concurrently as the control. Three replicates were included for each soil. Recovery rates were calculated using the following equation

$$\text{recovery}(\%) = \frac{T_m - T_0}{T_i} \times 100$$

where T_0 (NPs or ng) and T_m (NPs or ng) are NP contents in nonspiked control samples and in the soil spiked with a known content of HgS-NPs T_i (NPs or ng), respectively.

Quantification of Hg-NPs by Single Particle Inductively Coupled Plasma-Mass Spectrometry (spICP-MS). Hg-NP number/mass concentrations and size distributions were quantified by spICP-MS (single particle mode of Agilent 8800 triple quadrupole ICP-MS). The dwell time was 3 ms and the acquisition time was no less than 60 s.[17,20] Transport efficiency was determined using freshly prepared 30 nm AuNPs (30 ng L^{-1}; NanoComposix) in ultrapure water[29] and ranged from 4 to 6% for all experiments. Instrumental calibrations were obtained using freshly prepared mercury nitrate (Sigma-

https://doi.org/10.1021/acs.est.1c07039
Environ. Sci. Technol. 2022, 56, 1763−1770

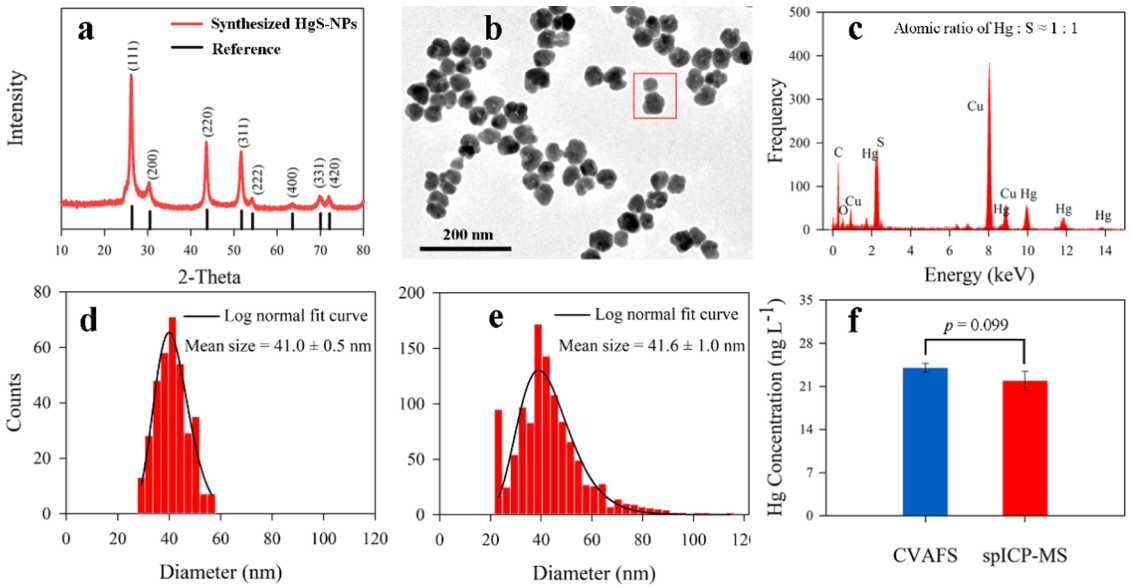

Figure 1. Characteristics of synthesized HgS-NPs. X-ray diffraction pattern of synthesized HgS-NPs (red line) and metacinnabar reference (black line) (a); representative TEM image of synthesized HgS-NPs (b); energy-dispersive X-ray spectroscopy in the selected area of panel (b) (c); size distribution of synthesized HgS-NPs in ultrapure water collected from TEM images (350 particles) (d); size distribution of synthesized HgS-NPs in ultrapure water analyzed by spICP-MS (e); and total mercury concentrations of synthesized HgS-NPs in ultrapure water determined by spICP-MS and cold-vapor atomic fluorescence spectroscopy (CVAFS) (f). Error bars represent the standard deviation of triplicates.

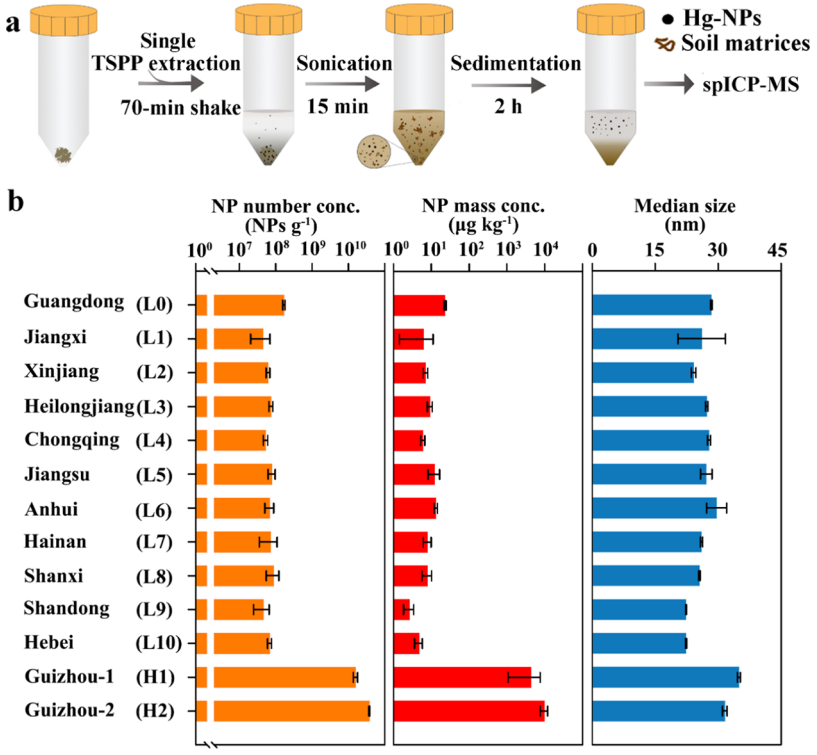

Figure 2. Extraction and quantification of indigenous Hg-NPs in natural soils. Schematic diagram for extraction and quantification of indigenous Hg-NPs in natural soil (a). Particle number/mass concentrations and median size of indigenous Hg-NPs in different soils (b). Note that these soils were not spiked with synthesized HgS-NPs. Data are shown as mean ± SD (n = 3).

Aldrich) at 1 μg L^{-1} in 2% HCl. Immediately before spICP-MS analysis, extracted soil samples were diluted 100−110 000 fold using ultrapure water, followed by 5 min sonication in a water bath (KQ-600E, China) to ensure uniform particle distribution. Typical instrumental parameters are given in Table S2.

For quality control, sample flow rate, transport efficiency, and mercury sensitivity were monitored every 10 samples. The memory effect of mercury was minimized using a sequential washing procedure after each sample measurement, i.e., acid mixture of 1% HCl and 2% HNO_3, 2% HNO_3, and finally ultrapure water.

All collected data were analyzed with Agilent Mass Hunter 4.5 Software, which identifies particle events using a 5σ methodology.[19] The frequency of particle events over the total

https://doi.org/10.1021/acs.est.1c07039
Environ. Sci. Technol. 2022, 56, 1763−1770

acquisition time is directly related to particle number concentration, and the intensity of the particle event is proportional to particle mass concentration with the knowledge of particle chemical composition.[22] Particle sizes were determined by assuming that (i) all particles were spherical (Figures 1b, S8, and S9) and (ii) the chemical composition is HgS with a density of 8.1 g cm^{-3} based on the results of X-ray absorption spectroscopy (Figure 4), which provide a simple pathway to roughly determine the particle size. In this study, the particle number detection limit was 1.2×10^5 NPs L^{-1} within 60 s acquisition time (see details in Text S1). The size detection limit was determined by background noise in ultrapure water (i.e., instrumental detection limit) and in extracted samples (i.e., method detection limit) (Text S1). Compared to an instrumental size detection limit of 21 nm, the method size detection limit ranges from 21 to 27 nm among tested soils, affected by the soil matrices (e.g., background mercury levels[30]).

Characterization of Hg-NPs Extracted from Natural Soils. Because NPs in soils L0−L10 were in the lower-to-sub-μg g^{-1} range, synchrotron-based X-ray analysis could not be directly applied to soils L0−L10 for supplementary investigations; transmission electron microscopy was only performed on the extracted Hg-NPs from soil L0 after preconcentration and those from soil H1 without preconcentration.

To determine the morphology, size, and elemental composition of Hg-NPs, TEM-EDS was performed in soils L0 and H1. Hg-NPs were extracted with the proposed method (Figure 2a) and sonicated for 5 min, and ∼5 μL aliquots were loaded onto 230-mesh carbon-coated copper grids. For soil L0, the extracted Hg-NPs were further preconcentrated using repetitive cloud point extraction for 15 cycles before TEM-EDS measurements.[31,32] A FEI Tecnai G2 F20 S-Twin high-resolution TEM (HR-TEM) was operated with a Schottky field emission gun at an acceleration voltage of 200 kV. Elemental composition in the selected areas was analyzed using EDS (Aztec X-Max 150, Oxford).

Speciation of mercury in the extracted H2 sample was analyzed at the Hg L_3-edge on beamline 20-BM of the Advanced Photon Source (APS; Illinois) using the multielement Ge detector placed at 45°. The extracted H2 sample was freeze-dried, ground into fine powders (<200 meshes), and packed into a 2-mm-thick Teflon sample holder sealed with a Kapton tape. Cinnabar (α-HgS), metacinnabar (β-HgS), $HgCl_2$, Hg(cysteine)$_2$ (representing organic Hg(SR)$_2$ species), Hg_2Cl_2, and HgO served as references.

Linear combination fit (LCF) of the normalized X-ray absorption near-edge structure (XANES) spectrum was conducted in the energy range of −30 to 120 eV relative to 12 284 eV using ATHENA[33] based on the spectra of samples and references (Figure S2). Extended X-ray absorption fine structure (EXAFS) spectrum modeling was performed in ARTEMIS following a previous method.[34] Atomic structures for EXAFS modeling were obtained from the American Mineralogist Crystal Structure Database.[35] The amplitude reduction factor (S_0^2) was obtained during the refinement of the first shell for β-HgS with a fixed coordination number (CN). On the basis of S_0^2, a static disorder value (σ^2) for each path, *CN*s, and the interatomic distance (R) of unknown samples were then obtained.

Mercury Analysis. Total Hg concentrations in air-dried soils were determined by direct thermal decomposition, amalgamation, and atomic absorption spectroscopy according to USEPA Method 7473 using Milestone DMA-80. Total Hg concentrations in the extracted samples were analyzed by cold-vapor atomic fluorescence spectroscopy (CVAFS, Brooks Rand, Seattle, WA) following USEPA Method 1631. Methylmercury in soils was determined by CVAFS following USEPA Method 1630. Approximately 0.5 g of soil was digested with 2 mL of 25% (w/w) KOH-CH_3OH for 4 h at 60 °C. The digests were diluted with 10 mL of ultrapure water, centrifuged (2000*g*, 30 min), and separated for the aqueous phase. The aqueous phase was ethylated by freshly thawed $NaBEt_4$ in citrate buffer (pH 4.1−4.5) for MeHg analysis. Certified reference materials for total Hg (GBW07405, National Research Center for Certified Reference Materials, China) and MeHg (estuarine sediment ERM-CC580, Institute for Reference Materials and Measurements, Belgium) and digestion blanks were measured for quality assurance and quality control. The recoveries were 83−88% for total Hg and 98−106% for MeHg.

Data Processing. Statistical significance between groups was calculated using the independent-samples T test ($p < 0.05$). The correlation of Hg-NP number concentrations to soil properties was evaluated using the Spearman's rank correlation coefficient (Spearman's rho).

RESULTS AND DISCUSSION

Characterization of Synthesized HgS-NPs. Synthesized HgS-NPs were characterized for the crystalline structure, size, shape, and elemental composition. XRD confirmed the formation of metacinnabar (β-HgS), with diffraction peaks at 26.38, 43.76, and 51.83°, corresponding to the β-HgS lattice plane of (111), (220), and (311) (Figure 1a). Natural occurrence of β-HgS has been observed in soils and sediments.[1,36−39] TEM analysis revealed that these HgS-NPs were spherical with the mean size of 41.0 ± 0.5 nm (350 particles; Figure 1b,d). EDS analysis showed that the Hg-to-S ratio was nearly 1:1, consistent with the stoichiometry of HgS (Figure 1b,c).

The mean size of nanoparticles determined by spICP-MS was 41.6 ± 1.0 nm (Figure 1e), comparable to the TEM size. The calculated mass concentration of HgS-NPs (21.9 ± 1.5 ng L^{-1}) was comparable to that determined by CVAFS (24.0 ± 0.7 ng L^{-1}; Figure 1f).

Extraction of Spiked HgS-NPs. Particle number/mass concentrations and size distribution are key factors affecting the biogeochemical behaviors of NPs. To this end, a screening test was performed to investigate the effects of different extraction reagents in the soil L0 sample amended with spiked HgS-NPs. As shown in Figure S3a, TSPP was the most effective reagent at liberating HgS-NPs. Moreover, 10 mM TSPP showed the greatest recovery performance, with particle number- and mass-based recoveries of 102 ± 1 and 104 ± 1%, respectively (Figure S3b). Further increase in TSPP concentration reduced the recovery, probably as a result of increased aggregation and adsorption of NPs at high ionic strength.[19] Neither extraction reagents nor TSPP concentrations led to significant shift in the size distributions of HgS-NPs when compared to their pristine counterparts in ultrapure water (Figure S3c). Note that the *in situ* formation of Hg-NPs in soil L0 by, for instance, soil organic matter[3,40] was unlikely (Figure S4). Moreover, aging time (24 h vs 30 days) had minimal effect on the performance of the extraction method (Figures S3b and S5). Thus, 10 mM TSPP was adopted for Hg-NP

https://doi.org/10.1021/acs.est.1c07039
Environ. Sci. Technol. 2022, 56, 1763−1770

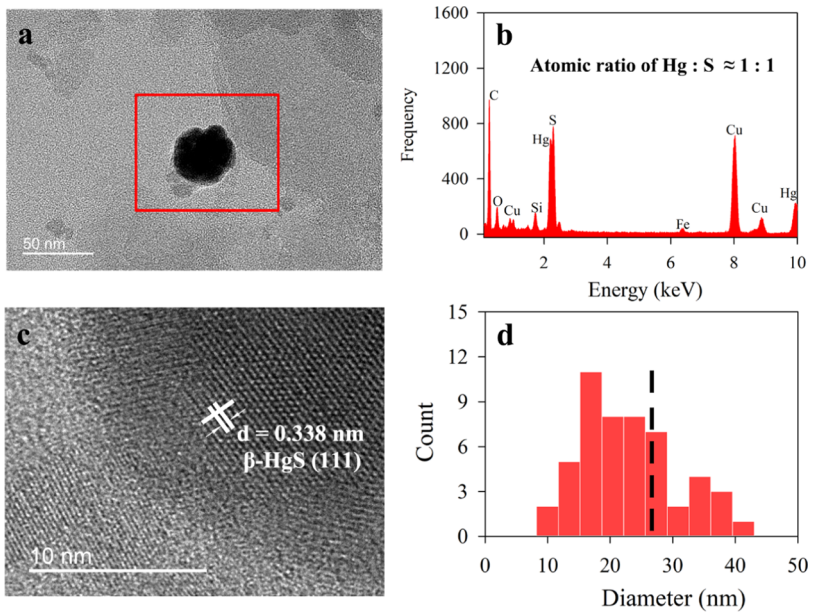

Figure 3. Characteristics of HgS-NPs extracted from the H1 sample using TEM coupled with energy-dispersive X-ray spectroscopy (EDS). Representative TEM image (a); EDS analysis of nanoparticles in the selected area in panel (a) (b); high-resolution TEM image of the selected area in panel (a) (c); and size distribution of HgS-NPs in the extracted H1 sample based on TEM analysis (n = 63) (d). Dashed line indicates a particle size of 27 nm.

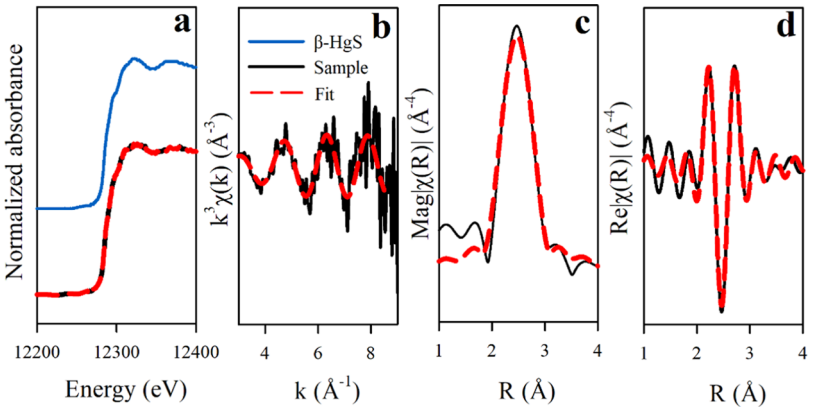

Figure 4. Speciation of mercury in the extracted H2 sample assessed by Hg L_3-edge XANES and EXAFS spectra. Normalized spectra of reference compounds β-HgS and the sample (a). Linear combination fit indicates that 72 ± 5% of total mercury was β-HgS (also see Table S3). k^3-weighted χ spectra (b), Fourier transform magnitude spectra (c), and Fourier transform real part spectra (d). The best fits of EXAFS are given by red dashed lines.

extraction from soils because it provided the highest particle number- and mass-based recoveries.

Recovery of Spiked HgS-NPs across Soils. The applicability of the proposed method was validated by examining other 12 soils with a wide variation in soil properties, e.g., pH (5.10−8.28; Table S1), soil organic matter content (SOM; 11.6−57.1 g kg^{-1}; Table S1), and total Hg concentrations (0.01−357.1 mg kg^{-1}; Table S1). Recovery rates for particle number, particle mass, and total Hg mass were 90−120, 74−113, and 89−115% for all soils, respectively (Figure S6a). Meanwhile, the measured size of extracted Hg-NPs across different soils agreed well with that of pristine spiked HgS-NPs (TEM size = 41.0 ± 0.5 nm; Figure S6b). Further, the particle number concentrations and size distributions were comparable between single extraction and repeated extraction (p > 0.05, Figure S7). This information allowed us to draw the conclusion that the proposed method is effective for quantifying Hg-NPs in complex soil matrices.

There is no historical record of recovery values of spiked HgS-NP number/mass concentrations in soils and sediments for direct comparison. TSPP extraction coupled with spICP-MS was previously performed in soils spiked with AgNPs and Ag_2S-NPs.[17,19,41] Particle mass- and number-based recoveries were 70−106 and 65−100% using 2.5 mM TSPP,[17,19] and 90−120% of particulate Ag mass was recovered using 10 mM TSPP.[41] These results collectively illustrated the potential of TSPP extraction coupled with spICP-MS for the quantitative analysis of silver- and mercury-based NPs in soils, as it provided information on particle number/mass concentrations and size distributions in soils at environmentally relevant concentrations.

Indigenous Hg-NPs across Natural Soils. Indigenous Hg-NPs in natural soils without spiked HgS-NPs were

https://doi.org/10.1021/acs.est.1c07039
Environ. Sci. Technol. 2022, 56, 1763−1770

characterized by high-resolution TEM-EDS and X-ray absorption spectroscopy. TEM-EDS analysis detected Hg-NPs in soil H1 (n = 63) and L0 (n = 5) (Figures S8 and S9). Spherical Hg-NPs were observed in soil H1 (43/63; see representative images in Figure S9) and L0 (4/5; Figure S8), and EDS analysis of most nanoparticles showed Hg-to-S ratios of nearly 1:1 (0.90 ± 0.40; Figure 3a,b). Moreover, high-resolution TEM demonstrated that these Hg-NPs had a characteristic d-spacing of 0.338 nm (Figure 3c), corresponding to the (111) lattice plane of β-HgS.[3,42] The mercury speciation of Hg-NPs in the extracted H2 sample was examined by the Hg L_3-edge X-ray absorption near-edge structure (XANES) and extended X-ray absorption fine structure (EXAFS) spectra. Linear combination fit (LCF) of the XANES spectrum indicated that the sample had a best fit for a mix with metacinnabar (β-HgS, 72 ± 5%) and $Hg(cysteine)_2$ (23 ± 5%) (R-factor = 0.001; Figure 4a and Table S3). The best fit of the EXAFS spectrum showed a Hg−S distance at 2.47 ± 0.01 Å (R-factor = 0.011; Figure 4b−d and Table S4), similar to that in β-HgS (~2.52Å).[43] Together, these results indicated that β-HgS was the major Hg species in extracted H1 and H2 samples. This is consistent with Yin et al.,[36] who found that 64−81% of total Hg was β-HgS in soils of the Wanshan mining area.

Based on the particle characteristics of indigenous Hg-NPs measured by TEM-EDS and X-ray absorption spectroscopy, volume equivalent spherical diameters and particle number/mass concentrations were determined by spICP-MS. Hg-NPs were of sizes from 21 to 120 nm (Figures S10 and 2b). NP concentrations varied substantially across soils. The number concentrations of Hg-NPs ranged from 10^7 to 10^9 NPs g^{-1} (dw) in soils L0−L10, and 1.6 (± 0.2) × 10^{10} and 3.7 (± 0.3) × 10^{10} NPs g^{-1} (dw) for soils H1 and H2, respectively (Figure 2b). Interestingly, the number concentrations of Hg-NPs were positively associated with the contents of soil organic matter and total Hg levels (p < 0.05; Table S5). The averaged mass concentrations of Hg-NPs were 2.6−22.9, 4346.6 ± 189.2, and 9782.0 ± 2124.7 μg kg^{-1} in soils L0−L10, H1, and H2, respectively. As a result, the proportion of indigenous Hg-NPs reached 3−40% of total mercury among tested soils (Table S1).

It is impossible to test the extraction recovery of indigenous Hg-NPs. However, our confidence derives from (i) satisfied recovery rates of spiked HgS-NPs, which aged in soils for 24 h and 30 days (Figures S3b and S5); (ii) comparable size distributions and particle number concentrations of indigenous HgS-NPs in soil H1 between single extraction and repeated extraction (Figure S7); and (iii) comparable size distribution of indigenous HgS-NPs determined by spICP-MS and TEM-EDS in soil H1 (see below).

TEM-EDS analysis revealed similar size distribution for particles larger than 27 nm in the H1 sample when compared to spICP-MS results (Figures 3d and S7b). Among the HgS-NPs visualized by TEM, ~40% were larger than 27 nm (Figure 3d). These nanoparticles had a median TEM size of 33.9 nm, similar to those measured by spICP-MS (35.0 nm; Figure 2b). However, we find that HgS-NPs were in the range of 27−120 nm by spICP-MS analysis (Figure S7b) but 8−43 nm by TEM-EDS analysis (n = 63; Figure 3d and also see examples in Figure S9). The difference is likely because (i) only a small fraction of the soil sample could be analyzed by TEM, and the low number of NPs (n = 63) reduced the statistical coverage and (ii) spICP-MS failed to adequately define small NPs below the method size detection limit of 27 nm for soil H1. There was a significant overlap in size distributions of particles within 27−43 nm, which accounted for ~40% of particles based on TEM-EDS analysis (Figure 3d), and these particles were 1.2 × 10^{10} NPs g^{-1} according to spICP-MS results. We then estimated that the particle number concentration of HgS-NPs within 8−27 nm was ~1.8 × 10^{10} NPs g^{-1}. After correction with TEM-EDS results, the indigenous HgS-NPs sized 8−120 nm were about 3.4 × 10^{10} NPs g^{-1} in soil H1. The low number of Hg-NPs in soil L0 (n = 5) observed by TEM-EDS prevented the validation of the particle size by spICP-MS. Therefore, further effort is needed to confirm the accuracy of size distribution.

These values are only tentative estimates, but indicate that the absence of smaller NPs below method size detection limits of spICP-MS (e.g., <27 nm for soil H1) can result in underestimated number concentrations in natural soils. This limitation could be addressed by combining with a variety of techniques such as electron microscopy analysis, as shown here, and by improving the size detection limit of spICP-MS via reducing the background noise and dissolved signal intensity, e.g., coupled to ion exchange resins.[44] This is critical for a more accurate quantification of particle number concentration and size distribution. Further progress is likely from the novel approaches such as time-of-flight mass spectrometry that could detect multiple elements per particle (Xu et al.[1]).

Environmental Implications. Here, we demonstrate the experimental determinations of indigenous Hg-NPs in natural soils. Although the mass concentrations of Hg-NPs are low (3−40% of total Hg), the huge number concentrations of these NPs (between 10^7 and 10^{11} NP g^{-1}) requires serious attention. The knowledge of particle number/mass concentrations, along with the size, can lead to a more complete understanding of the fate of geochemical intermediates of mercury (i.e., Hg-NPs).

Importantly, indigenous Hg-NPs in natural soils may pose a risk to environmental health. It has been documented that methylation potentials of spiked HgS-NPs are ~2% in uncontaminated soil at 0.3 mg Hg kg^{-1} and ~0.004% in Wanshan soil at 48.4 mg Hg kg^{-1}.[45] Assuming that the activity of microbial methylators is not a limiting factor for mercury methylation in all tested soils, we estimate that between 0.09 and 0.46 μg MeHg kg^{-1} would be produced based on indigenous Hg-NP concentrations in soils L0−L10 (2.6−22.9 μg kg^{-1}). Thus, 12−65% of measured MeHg in these soils might originate from Hg-NP methylation (Table S1). Analogically, indigenous Hg-NPs in Wanshan mining soils (4346.6−9782.0 μg kg^{-1}) appear to contribute to 5−16% of measured MeHg (Table S1). Nevertheless, due to the low percentage of Hg-NPs in Wanshan mining soils (Table S1), low abundance of mercury methylation genes (i.e., hgcA and hgcB), and high demethylation rate,[45,46] less contribution of Hg-NPs to MeHg production in Wanshan mining soils was observed.

Overall, the proposed method can provide detailed information on Hg-NP number/mass concentrations and size, which will not only strengthen our understanding of mercury methylation processes governing the public exposure to MeHg but also guide further studies focusing on the biogeochemical cycling of Hg-NPs.

https://doi.org/10.1021/acs.est.1c07039
Environ. Sci. Technol. 2022, 56, 1763−1770

■ ASSOCIATED CONTENT

Supporting Information

The Supporting Information is available free of charge at https://pubs.acs.org/doi/10.1021/acs.est.1c07039.

Details about the detection limit of spICP-MS, experimental procedure, performance of the proposed extraction method, TEM-EDS results of soils L0 and H1, size distributions of indigenous Hg-NPs in natural soils, properties of sampled soils, typical instrument parameters for spICP-MS analysis, XAS modeling results, and correlations between Hg-NP number concentration and soil properties (PDF)

■ AUTHOR INFORMATION

Corresponding Author

Fei Dang − *Key Laboratory of Soil Environment and Pollution Remediation, Institute of Soil Science, Chinese Academy of Sciences, Nanjing 210008, China; University of Chinese Academy of Sciences, Beijing 100049, China;* orcid.org/0000-0002-2989-9916; Email: fdang@issas.ac.cn

Authors

Weiping Cai − *Key Laboratory of Soil Environment and Pollution Remediation, Institute of Soil Science, Chinese Academy of Sciences, Nanjing 210008, China; University of Chinese Academy of Sciences, Beijing 100049, China*

Yujun Wang − *Key Laboratory of Soil Environment and Pollution Remediation, Institute of Soil Science, Chinese Academy of Sciences, Nanjing 210008, China; University of Chinese Academy of Sciences, Beijing 100049, China;* orcid.org/0000-0002-0921-0122

Yu Feng − *School of Environmental Studies, China University of Geosciences, Wuhan 430074, China*

Peng Liu − *School of Environmental Studies, China University of Geosciences, Wuhan 430074, China;* orcid.org/0000-0002-2870-7193

Shuofei Dong − *Agilent Technologies Co., Ltd (China), Beijing 100102, China*

Bo Meng − *State Key Laboratory of Environmental Geochemistry, Institute of Geochemistry, Chinese Academy of Sciences, Guiyang 550002, China;* orcid.org/0000-0002-7827-8673

Hua Gong − *Key Laboratory of Soil Environment and Pollution Remediation, Institute of Soil Science, Chinese Academy of Sciences, Nanjing 210008, China*

Complete contact information is available at: https://pubs.acs.org/10.1021/acs.est.1c07039

Notes

The authors declare no competing financial interest.

■ ACKNOWLEDGMENTS

The authors thank the anonymous reviewers for their comments. The authors are grateful to the Advanced Photon Source, Argonne National Laboratory, for performing X-ray absorption spectroscopy analysis at Beamline 20-BM. This work was supported by the Youth Innovation Promotion Association, Chinese Academy of Sciences (2020314) and the National Natural Science Foundation of China (41977355).

■ REFERENCES

(1) Xu, J.; Bland, G. D.; Gu, Y.; Ziaei, H.; Xiao, X.; Deonarine, A.; Reible, D.; Bireta, P.; Hoelen, T. P.; Lowry, G. V. Impacts of Sediment Particle Grain Size and Mercury Speciation on Mercury Bioavailability Potential. *Environ. Sci. Technol.* **2021**, *55*, 12393−12402.

(2) O'Connor, D.; Hou, D.; Ok, Y. S.; Mulder, J.; Duan, L.; Wu, Q.; Wang, S.; Tack, F. M. G.; Rinklebe, J. Mercury speciation, transformation, and transportation in soils, atmospheric flux, and implications for risk management: A critical review. *Environ. Int.* **2019**, *126*, 747−761.

(3) Manceau, A.; Lemouchi, C.; Enescu, M.; Gaillot, A.-C.; Lanson, M.; Magnin, V.; Glatzel, P.; Poulin, B. A.; Ryan, J. N.; Aiken, G. R.; et al. Formation of mercury sulfide from Hg (II)−thiolate complexes in natural organic matter. *Environ. Sci. Technol.* **2015**, *49*, 9787−9796.

(4) Lin, Y.; Larssen, T.; Vogt, R. D.; Feng, X. Identification of fractions of mercury in water, soil and sediment from a typical Hg mining area in Wanshan, Guizhou province, China. *Appl. Geochem.* **2010**, *25*, 60−68.

(5) Deonarine, A.; Hsu-Kim, H. Precipitation of Mercuric Sulfide Nanoparticles in NOM-Containing Water: Implications for the Natural Environment. *Environ. Sci. Technol.* **2009**, *43*, 2368−2373.

(6) Wolfenden, S.; Charnock, J. M.; Hilton, J.; Livens, F. R.; Vaughan, D. J. Sulfide species as a sink for mercury in lake sediments. *Environ. Sci. Technol.* **2005**, *39*, 6644−6648.

(7) Zhang, T.; Kucharzyk, K. H.; Kim, B.; Deshusses, M. A.; Hsu-Kim, H. Net methylation of mercury in estuarine sediment microcosms amended with dissolved, nanoparticulate, and microparticulate mercuric sulfides. *Environ. Sci. Technol.* **2014**, *48*, 9133−9141.

(8) Cai, W.; Jin, J.; Dang, F.; Shi, W.; Zhou, D. Mercury methylation from mercury selenide particles in soils. *J. Hazard. Mater.* **2020**, *400*, No. 123248.

(9) Tian, L.; Guan, W.; Ji, Y.; He, X.; Chen, W.; Alvarez, P. J. J.; Zhang, T. Microbial methylation potential of mercury sulfide particles dictated by surface structure. *Nat. Geosci.* **2021**, *14*, 409−416.

(10) Rivera, N. A., Jr; Bippus, P. M.; Hsu-Kim, H. Relative reactivity and bioavailability of mercury sorbed to or coprecipitated with aged iron sulfides. *Environ. Sci. Technol.* **2019**, *53*, 7391−7399.

(11) Graham, A. M.; Aiken, G. R.; Gilmour, C. C. Dissolved organic matter enhances microbial mercury methylation under sulfidic conditions. *Environ. Sci. Technol.* **2012**, *46*, 2715−2723.

(12) Thomas, S. A.; Rodby, K. E.; Roth, E. W.; Wu, J.; Gaillard, J.-F. Spectroscopic and microscopic evidence of biomediated HgS species formation from Hg (II)−cysteine complexes: implications for Hg (II) bioavailability. *Environ. Sci. Technol.* **2018**, *52*, 10030−10039.

(13) Gray, E. P.; Coleman, J. G.; Bednar, A. J.; Kennedy, A. J.; Ranville, J. F.; Higgins, C. P. Extraction and Analysis of Silver and Gold Nanoparticles from Biological Tissues Using Single Particle Inductively Coupled Plasma Mass Spectrometry. *Environ. Sci. Technol.* **2013**, *47*, 14315−14323.

(14) Rodrigues, S. M.; Trindade, T.; Duarte, A. C.; Pereira, E.; Koopmans, G. F.; Romkens, P. F. A. M. A framework to measure the availability of engineered nanoparticles in soils: Trends in soil tests and analytical tools. *TrAC, Trends Anal. Chem.* **2016**, *75*, 129−140.

(15) Monikh, F. A.; Chupani, L.; Vijver, M. G.; Vancova, M.; Peijnenburg, W. J. G. M. Analytical approaches for characterizing and quantifying engineered nanoparticles in biological matrices from an (eco)toxicological perspective: old challenges, new methods and techniques. *Sci. Total Environ.* **2019**, *660*, 1283−1293.

(16) Laborda, F.; Bolea, E.; Cepria, G.; Gomez, M. T.; Jimenez, M. S.; Perez-Arantegui, J.; Castillo, J. R. Detection, characterization and quantification of inorganic engineered nanomaterials: A review of techniques and methodological approaches for the analysis of complex samples. *Anal. Chim. Acta* **2016**, *904*, 10−32.

(17) Schwertfeger, D. M.; Velicogna, J. R.; Jesmer, A. H.; Saatcioglu, S.; McShane, H.; Scroggins, R. P.; Princz, J. I. Extracting Metallic Nanoparticles from Soils for Quantitative Analysis: Method Develop-

ment Using Engineered Silver Nanoparticles and SP-ICP-MS. *Anal. Chem.* **2017**, *89*, 2505−2513.
(18) Liu, W.; Shi, H.; Liu, K.; Liu, X.; Sahle-Demessie, E.; Stephan, C. A Sensitive Single Particle-ICP-MS Method for CeO_2 Nanoparticles Analysis in Soil during Aging Process. *J. Agric. Food Chem.* **2021**, *69*, 1115−1122.
(19) Li, L.; Wang, Q.; Yang, Y.; Luo, L.; Ding, R.; Yang, Z.-G.; Li, H.-P. Extraction Method Development for Quantitative Detection of Silver Nanoparticles in Environmental Soils and Sediments by Single Particle Inductively Coupled Plasma Mass Spectrometry. *Anal. Chem.* **2019**, *91*, 9442−9450.
(20) Tou, F.; Niu, Z.; Fu, J.; Wu, J.; Liu, M.; Yang, Y. Simple Method for the Extraction and Determination of Ti-, Zn-, Ag-, and Au-Containing Nanoparticles in Sediments Using Single-Particle Inductively Coupled Plasma Mass Spectrometry. *Environ. Sci. Technol.* **2021**, *55*, 10354−10364.
(21) Li, P.; Lv, F.; Xu, J.; Yang, K.; Lin, D. Separation and Analysis of Nanoscale Zero-Valent Iron from Soil. *Anal. Chem.* **2021**, *93*, 10187−10195.
(22) Laborda, F.; Bolea, E.; Jimenez-Lamana, J. Single Particle Inductively Coupled Plasma Mass Spectrometry: A Powerful Tool for Nanoanalysis. *Anal. Chem.* **2014**, *86*, 2270−2278.
(23) Pace, H. E.; Rogers, N. J.; Jarolimek, C.; Coleman, V. A.; Gray, E. P.; Higgins, C. P.; Ranville, J. F. Single Particle Inductively Coupled Plasma-Mass Spectrometry: A Performance Evaluation and Method Comparison in the Determination of Nanoparticle Size. *Environ. Sci. Technol.* **2012**, *46*, 12272−12280.
(24) Monikh, F. A.; Chupani, L.; Arenas-Lago, D.; Guo, Z.; Zhang, P.; Darbha, G. K.; Valsami-Jones, E.; Lynch, I.; Vijver, M. G.; van Bodegom, P. M.; Peijnenburg, W. J. G. M. Particle number-based trophic transfer of gold nanomaterials in an aquatic food chain. *Nat. Commun.* **2021**, *12*, No. 899.
(25) Zhu, J.-F.; Zhu, Y.-J.; Ma, M.-G.; Yang, L.-X.; Gao, L. Simultaneous and rapid microwave synthesis of polyacrylamide-metal sulfide (Ag_2S, Cu_2S, HgS) nanocomposites. *J. Phys. Chem. C* **2007**, *111*, 3920−3926.
(26) Zhang, H.; Feng, X.; Larssen, T.; Shang, L.; Li, P. Bioaccumulation of Methylmercury versus Inorganic Mercury in Rice (*Oryza sativa* L.) Grain. *Environ. Sci. Technol.* **2010**, *44*, 4499−4504.
(27) Ma, L.; Zhong, H.; Wu, Y.-G. Effects of Metal-Soil Contact Time on the Extraction of Mercury from Soils. *Bull. Environ. Contam. Toxicol.* **2015**, *94*, 399−406.
(28) Liang, X.; Lu, X.; Zhao, J.; Liang, L.; Zeng, E. Y.; Gu, B. Stepwise Reduction Approach Reveals Mercury Competitive Binding and Exchange Reactions within Natural Organic Matter and Mixed Organic Ligands. *Environ. Sci. Technol.* **2019**, *53*, 10685−10694.
(29) Pace, H. E.; Rogers, N. J.; Jarolimek, C.; Coleman, V. A.; Higgins, C. P.; Ranville, J. F. Determining Transport Efficiency for the Purpose of Counting and Sizing Nanoparticles via Single Particle Inductively Coupled Plasma Mass Spectrometry. *Anal. Chem.* **2011**, *83*, 9361−9369.
(30) Hadioui, M.; Knapp, G.; Azimzada, A.; Jreije, I.; Frechette-Viens, L.; Wilkinson, K. J. Lowering the Size Detection Limits of Ag and TiO_2 Nanoparticles by Single Particle ICP-MS. *Anal. Chem.* **2019**, *91*, 13275−13284.
(31) Zhou, X.-X.; Liu, J.-F.; Jiang, G.-B. Elemental Mass Size Distribution for Characterization, Quantification and Identification of Trace Nanoparticles in Serum and Environmental Waters. *Environ. Sci. Technol.* **2017**, *51*, 3892−3901.
(32) Urstoeger, A.; Wimmer, A.; Kaegi, R.; Reiter, S.; Schuster, M. Looking at Silver-Based Nanoparticles in Environmental Water Samples: Repetitive Cloud Point Extraction Bridges Gaps in Electron Microscopy for Naturally Occurring Nanoparticles. *Environ. Sci. Technol.* **2020**, *54*, 12063−12071.
(33) Ravel, B.; Newville, M. ATHENA, ARTEMIS, HEPHAESTUS: data analysis for X-ray absorption spectroscopy using IFEFFIT. *J. Synchrotron Radiat.* **2005**, *12*, 537−541.
(34) Liu, P.; Ptacek, C. J.; Elena, K. M. A.; Blowes, D. W.; Gould, W. D.; Finfrock, Y. Z.; Wang, A. O.; Landis, R. C. Evaluation of mercury stabilization mechanisms by sulfurized biochars determined using X-ray absorption spectroscopy. *J. Hazard. Mater.* **2018**, *347*, 114−122.
(35) Downs, R. T.; Hall-Wallace, M. The American mineralogist crystal structure database. *Am. Mineral.* **2003**, *88*, 247−250.
(36) Yin, R.; Gu, C.; Feng, X.; Hurley, J. P.; Krabbenhoft, D. P.; Lepak, R. F.; Zhu, W.; Zheng, L.; Hu, T. Distribution and geochemical speciation of soil mercury in Wanshan Hg mine: Effects of cultivation. *Geoderma* **2016**, *272*, 32−38.
(37) Kim, C. S.; Bloom, N. S.; Rytuba, J. J.; Brown, G. E. Mercury speciation by X-ray absorption fine structure spectroscopy and sequential chemical extractions: A comparison of speciation methods. *Environ. Sci. Technol.* **2003**, *37*, 5102−5108.
(38) Martín-Doimeadios, R. C. R.; Wasserman, J. C.; Bermejo, L. F. G.; Amouroux, D.; Nevado, J. J. B.; Donard, O. F. X. Chemical availability of mercury in stream sediments from the Almaden area, Spain. *J. Environ. Monitor.* **2000**, *2*, 360−366.
(39) Skyllberg, U.; Persson, A.; Tjerngren, I.; Kronberg, R.-M.; Drott, A.; Meili, M.; Bjorn, E. Chemical speciation of mercury, sulfur and iron in a dystrophic boreal lake sediment, as controlled by the formation of mackinawite and framboidal pyrite. *Geochim. Cosmochim. Ac.* **2021**, *294*, 106−125.
(40) Barnett, M. O.; Harris, L. A.; Turner, R. R.; Stevenson, R. J.; Henson, T. J.; Melton, R. C.; Hoffman, D. P. Formation of Mercuric Sulfide in Soil. *Environ. Sci. Technol.* **1997**, *31*, 3037−3043.
(41) Hong, A.; Tang, Q.; Khan, A. U.; Miao, M.; Xu, Z.; Dang, F.; Liu, Q.; Wang, Y.; Lin, D.; Filser, J.; Li, L. Identification and Speciation of Nanoscale Silver in Complex Solid Matrices by Sequential Extraction Coupled with Inductively Coupled Plasma Optical Emission Spectrometry. *Anal. Chem.* **2021**, *93*, 1962−1968.
(42) Zhang, Z.; Si, R.; Lv, J.; Ji, Y.; Chen, W.; Guan, W.; Cui, Y.; Zhang, T. Effects of Extracellular Polymeric Substances on the Formation and Methylation of Mercury Sulfide Nanoparticles. *Environ. Sci. Technol.* **2020**, *54*, 8061−8071.
(43) Avellan, A.; Stegemeier, J. P.; Gai, K.; Dale, J.; Hsu-Kim, H.; Levard, C.; O'Rear, D.; Hoelen, T. P.; Lowry, G. V. Speciation of Mercury in Selected Areas of the Petroleum Value Chain. *Environ. Sci. Technol.* **2018**, *52*, 1655−1664.
(44) Hadioui, M.; Peyrot, C.; Wilkinson, K. J. Improvements to Single Particle ICPMS by the Online Coupling of Ion Exchange Resins. *Anal. Chem.* **2014**, *86*, 4668−4674.
(45) Liu, J.; Lu, B.; Poulain, A. J.; Zhang, R.; Zhang, T.; Feng, X.; Meng, B. The underappreciated role of natural organic matter bond Hg(II) and nanoparticulate HgS as substrates for methylation in paddy soils across a Hg concentration gradient. *Environ. Pollut.* **2022**, *292*, No. 118321.
(46) Parks, J. M.; Johs, A.; Podar, M.; Bridou, R.; Hurt, R. A., Jr; Smith, S. D.; Tomanicek, S. J.; Qian, Y.; Brown, S. D.; Brandt, C. C.; et al. The genetic basis for bacterial mercury methylation. *Science* **2013**, *339*, 1332−1335.

https://doi.org/10.1021/acs.est.1c07039
Environ. Sci. Technol. 2022, 56, 1763−1770